

(ⁿBu₄N)[Ni(dmstfdt)₂]: A Planar Nickel Coordination Complex with an Extended-TTF Ligand Exhibiting Metallic Conduction, Metal–Insulator Transition, and Weak Ferromagnetism

Emiko Fujiwara,[†] Kimiko Yamamoto,[†] Mina Shimamura,[†] Biao Zhou,[‡]
Akiko Kobayashi,^{*,†,‡} Kazuyuki Takahashi,[§] Yoshinori Okano,[§] Hengbo Cui,[§] and
Hayao Kobayashi[§]

Research Centre for Spectrochemistry, Graduate School of Science, The University of Tokyo, Hongo, Bunkyo-ku, Tokyo 113-0033, Japan, Department of Chemistry, College of Humanities and Sciences, Nihon University, Sakurajosui, Setagaya-ku, Tokyo 156-8550, Japan, and Institute for Molecular Science and JST-CREST, Okazaki 444-8585, Japan

Received September 8, 2006. Revised Manuscript Received November 17, 2006

The 1:1 tetrabutylammonium salt of a nickel complex with an extended-TTF ligand, (ⁿBu₄N)[Ni(dmstfdt)₂] (dmstfdt = dimethyldiselenadithiafulvalenedithiolate) (**1**) is a unique ambivalent molecular system exhibiting weakly metallic conduction above room temperature and a weak ferromagnetism at low temperature. Its X-ray structure consists of two independent [Ni(dmstfdt)₂][−] (A and B) and two ⁿBu₄N⁺ in the unit cell. The pseudo-planar anions are arranged in a zigzag -ABA'B'- manner along the molecular side-by-side direction with a dihedral angle of the molecular planes of 42.6°. The tight-binding band structure calculation, based on transfer integrals estimated by the extended Hückel approximation, presents both three-dimensional electron and hole Fermi surfaces, which is consistent with the observed weakly metallic conduction around room-temperature despite the 1:1 stoichiometry of the complex. At 147 K, **1** shows a sharp insulating transition associated with the localization of one electron on each nickel complex below 160 K. The χT values of **1** increase linearly from 0.129 to 0.383 emu K mol^{−1} with decreasing temperature (160–340 K), suggesting a gradual electron localization with lowering the temperature. In the range of temperature of 80–150 K, χ follows the Curie–Weiss law: $\chi = C/(T - \theta)$; $C = 0.383$ emu K mol^{−1}; and $\theta = -4$ K. Weak ferromagnetism sets in below 20 K. The coercive field is ± 1.3 kOe at 2.0 K.

Introduction

The discovery of a single-component molecular metal, [Ni(tmtdt)₂] (tmtdt = trimethylenetetrafulvalenedithiolate), has defeated the preconception that crystals composed of only one kind of molecule should be insulators.^{1,2} Since [Ni(tmtdt)₂] has an even number of electrons, the system should have equal numbers of electrons and holes. Recently, however, experimental evidence for the three-dimensional electron and hole Fermi surfaces in [Ni(tmtdt)₂] was obtained by the observation of de Haas–van Alphen oscillations.³ On the other hand, the salts of monoanionic nickel complexes with analogous extended-TTF (tetrathiafulvalene) ligands (L) [NR₄][Ni(L)₂] will have an extra electron, and if the transfer integrals are as found in [Ni(tmtdt)₂], they should provide another type of interesting molecular conductor but

this time with a half-filled band already existing.^{4,5} It is widely believed that the molecular conductor with a half-filled narrow band tends to be an insulator because of an on-site Coulombic correlation effect (U). To our knowledge, the known exceptions are (TTM-TTP)I₃⁶ (TTM-TTP = 2,5-bis[4,5-bis(methylthio)-1,3-dithiol-2-ylidene]-1,3,4,6-tetrathiaapentalene), (DMTSA)NO₃ (DMTSA = 3,4-dimethylantra-[1,9-*cd*:4,10-*c'd'*]bis[1,2]-diselenole), and (DMTSA)BF₄,⁷ where close intermolecular contacts between these donor molecules are considered to yield large transfer integrals (t). Furthermore, in the special case of TTM-TTP, U is expected to be smaller than those of usual organic donors because of its extended π -conjugated electronic structure. Practically, the evaluation of U and t of (TTM-TTP)I₃ was performed by the measurement of polarized reflection spectra using a half-filled Hubbard model, resulting in that U was considered to be a little smaller than the bandwidth w ($\approx 4t$) ($U \approx 0.5$ eV and $t \approx 0.15$ eV).⁸ Even when these conditions are

* Corresponding author. Tel.: (+81)3-3329-1151 (ext. 5712). Fax: (+81) 3-3303-9899. E-mail: akoba@chs.nihon-u.ac.jp.

[†] The University of Tokyo.

[‡] Institute for Molecular Science and JST-CREST.

[§] Nihon University.

- (1) (a) Tanaka, H.; Okano, Y.; Kobayashi, H.; Suzuki, W.; Kobayashi, A. *Science* **2001**, *291*, 285. (b) Kobayashi, A.; Tanaka, H.; Kobayashi, H. *J. Mater. Chem.* **2001**, *11*, 2078.
- (2) Kobayashi, A.; Fujiwara, E.; Kobayashi, H. *Chem. Rev.* **2004**, *104*, 5243.
- (3) Tanaka, H.; Tokumoto, M.; Ishibashi, S.; Graf, D.; Choi, E. S.; Brooks, J. S.; Yasuzuka, S.; Okano, Y.; Kobayashi, H.; Kobayashi, A. *J. Am. Chem. Soc.* **2004**, *126*, 10518.

- (4) Coomber, A. T.; Beljonne, D.; Friend, R. H.; Brédas, J. L.; Charlton, A.; Robertson, N.; Underhill, A. E.; Kurmoo, M.; Day, P. *Nature* **1996**, *380*, 144.
- (5) Parker, I. D.; Friend, R. H.; Clemenson, P. I.; Underhill, A. E. *Nature* **1986**, *324*, 547.
- (6) Mori, T.; Inokuchi, H.; Misaki, Y.; Inabe, T.; Mori, H.; Tanaka, S. *Bull. Chem. Soc. Jpn.* **1994**, *67*, 661.
- (7) Takimiya, K.; Ohnishi, A.; Aso, Y.; Otsubo, T.; Ogura, F.; Kawabata, K.; Tanaka, K.; Mizutani, M. *Bull. Chem. Soc. Jpn.* **1994**, *67*, 766.

satisfied, the metallic conduction of the previously mentioned three 1:1 salts remains but only above 160, 220, and 160 K, respectively. In the case of the molecular conductors based on transition metal complexes with extended-TTF ligands, it might be possible that the magnitude of U can be strongly reduced by accommodating two excess electrons separately as far as possible in the left and right ligand moieties. Then, the effective U will become comparable to the Coulombic repulsion between neighboring TTF-like molecules (V) because the shortest S...S distance between sulfur atoms of the left and right ligands is about 3.0 Å. Therefore, the electrons in these systems will be much more mobile as compared with usual highly correlated organic conductors even when t is not so large. In addition to the small U , there is another important aspect in the electronic band structure of $[\text{NR}_4][\text{Ni}(\text{L})_2]$. A very small HOMO-LUMO gap of the transition metal complex with extended TTF ligands also makes the electronic structure very attractive because it suggests the possibility of mixing the HOMO and LUMO bands.^{2,9}

To obtain a new class of molecular metals, we have synthesized and examined a 1:1 nickel complex with TTF-type ligands (more precisely, STF (diselenadithiafulvalene)-type ligands), $(^n\text{Bu}_4\text{N})[\text{Ni}(\text{dmstfdt})_2]$ (dmstfdt = dimethyl-diselenadithiafulvalenedithiolate) (**1**).

Experimental Procedures

General. 4,5-Bis(2'-cyanoethylthio)-4,5-dimethyl-STF (**2**) was synthesized according to the method described in a previous paper.¹⁰ Tetrahydrofuran was freshly distilled over sodium and benzophenone under argon atmosphere prior to use. Methanol was distilled over magnesium methoxide under argon atmosphere. $\text{NiCl}_2 \cdot 6\text{H}_2\text{O}$ was recrystallized several times from distilled water and dried in vacuo. Supporting electrolyte of $^n\text{Bu}_4\text{N} \cdot \text{PF}_6$ was recrystallized several times from ethanol and dried in vacuo. Acetonitrile was distilled in the presence of calcium hydride under an argon atmosphere. All other reagents were used without purification.

Synthesis of $(^n\text{Bu}_4\text{N})[\text{Ni}(\text{dmstfdt})_2]$ (1**).** The STF derivative **2** (248 mg; 0.50 mmol) was hydrolyzed with a 25 wt % methanol solution of tetramethylammonium hydroxide (732 mg; 2.0 mmol) in dry tetrahydrofuran (15.0 mL) at room temperature and under argon atmosphere. The solution was stirred for 30 min, and $(\text{Me}_4\text{N})_2\text{-dmstfdt}$ precipitated out. A solution of $\text{NiCl}_2 \cdot 6\text{H}_2\text{O}$ (64.0 mg; 0.27 mmol) in methanol (4.0 mL) was added dropwise to the reaction mixture at -78°C , and the reaction mixture was stirred for 1 h at -78°C and then warmed to room temperature overnight. The resulting microcrystals were collected by filtration and washed several times with a mixed solvent of tetrahydrofuran (5.0 mL) and methanol (1.0 mL) under an argon atmosphere to afford reddish-brown microcrystals **3**, $(\text{Me}_4\text{N})_2[\text{Ni}(\text{dmstfdt})_2]$. The preparation of **1** was carried out electrochemically in a standard H-type cell without a glass-frit using two platinum electrodes (1 mm ϕ wires) under an argon inert atmosphere. The complex **3** (15.0–20.0 mg; 1.8×10^{-2} to 2.4×10^{-2} mmol) and $^n\text{Bu}_4\text{N} \cdot \text{PF}_6$ (80.0 mg; 234 mmol) were dissolved in acetonitrile (15.0 mL) under an argon atmosphere.

After filtration of precipitates, electrochemical oxidation of the obtained reddish-purple solution was carried out under a constant current of 0.2 μA at room temperature. Comparatively, the air-stable plate-shaped dark brown single crystals of **1** grew on the anode within about 3–4 weeks. The obtained crystals were filtered, washed with ethanol, and air-dried at room temperature. As the solubility of the selenium-containing metal complexes is usually lower than that of the corresponding sulfur analogues, the solubility of **1** to organic solvents is low, and the 1:1 complex grew on the anode without further oxidation to the neutral complex.

Crystal Structure Determination. The crystal structure determination of **1** was carried out at room temperature using a Rigaku AFC-8 Mercury CCD system equipped with graphite monochromated Mo K α radiation ($\lambda = 0.7107$ Å) and a confocal X-ray mirror. A tiny plate-shaped crystal with dimensions of about 0.10 mm \times 0.07 mm \times 0.02 mm was used. Crystal data at 293 K were as follows: $\text{C}_{32}\text{H}_{48}\text{NNiS}_8\text{Se}_4$, $M = 1077.76$; triclinic; space group $P\bar{1}$ (No. 2); $a = 19.541(9)$, $b = 8.661(3)$, and $c = 26.660(11)$ Å; $\alpha = 90.715(7)$, $\beta = 110.509(9)$, and $\gamma = 92.601(7)^\circ$; $V = 4219.9(31)$ Å³; $Z = 4$; $d_{\text{calcd}} = 1.696$ g cm⁻³; $\mu = 43.31$ cm⁻¹; and $F_{000} = 2156.00$. The number of collected reflections was 33474. The structure was solved by direct methods (SIR97).¹¹ The atomic scattering factors were taken from the International Tables for X-ray Crystallography. The non-hydrogen atoms were anisotropically refined by full-matrix least-squares method based on 6843 observed reflections [$I > 3.5\sigma(I)$] and 925 variable parameters. The final R and GOF values were $R = 0.061$, $R_w = 0.070$, and $\text{GOF} = 1.131$. All the calculations were performed using the CrystalStructure crystallographic software package.¹²

Electrical Resistivity Measurement. The four-probe electrical resistivity measurements were performed on **1** down to liquid nitrogen temperature by using a Huso Electro Chemical System HECS 944C multichannel four-terminal conductometer. Electrical contacts were made with gold wire (10 μm ϕ) and gold paste.

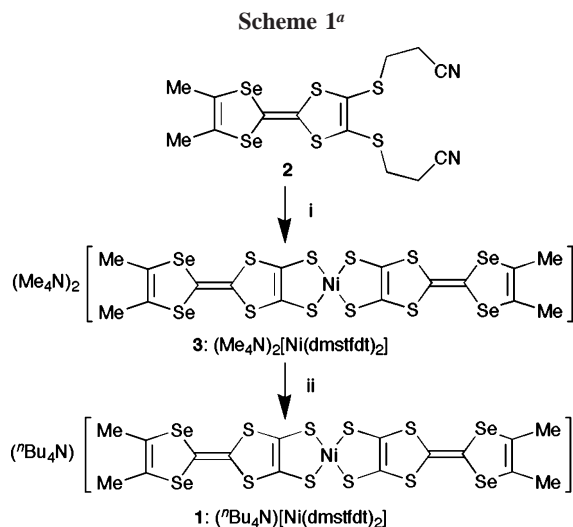
Magnetic Susceptibility Measurement. The magnetic susceptibility of polycrystalline sample **1** was measured using a Quantum Design MPMS-2 SQUID magnetometer in the temperature range from 2.0 to 340 K under various magnetic fields. The samples (2.52 mg; 1.2×10^{-3} mmol) were wrapped with clean aluminum foil whose magnetic susceptibility was separately measured and subtracted. The data were corrected for the diamagnetic contribution estimated from Pascal's constants ($\chi^{\text{dia}} = -5.43 \times 10^{-4}$ emu mol⁻¹).

Results and Discussion

Synthesis of $(^n\text{Bu}_4\text{N})[\text{Ni}(\text{dmstfdt})_2]$ (1**).** The syntheses of the dimethyl-STF dithiolate ligands, and the corresponding metal complex, were performed under a strictly inert atmosphere using the Schlenk technique according to the published methods (Scheme 1).^{1,2,10,13} The 2:1 salt, $(\text{Me}_4\text{N})_2[\text{Ni}(\text{dmstfdt})_2]$ (**3**), was obtained as an air unstable reddish-brown powder by the deprotection of dimethyl-STF dithiolate substituted with two 2-cyanoethylthio groups **2** using a 25 wt % $\text{Me}_4\text{N} \cdot \text{OH}$ /methanol solution in dry tetrahydrofuran, followed by the reaction of a $\text{NiCl}_2 \cdot 6\text{H}_2\text{O}$ /methanol solution at temperatures from -78°C to room temperature. An electrochemical oxidation of **3** was performed in the presence

- (8) Tajima, H.; Arifuku, M.; Ohta, T.; Mori, T.; Misaki, Y.; Yamabe, T.; Mori, H.; Tanaka, S. *Synth. Met.* **1995**, *71*, 1951.
 (9) Kobayashi, A.; Sasa, M.; Suzuki, W.; Fujiwara, E.; Tanaka, H.; Tokumoto, M.; Okano, Y.; Fujiwara, H.; Kobayashi, H. *J. Am. Chem. Soc.* **2004**, *126*, 426.
 (10) Binet, L.; Fabre, J. M.; Montginoul, C.; Simonsen, K. B.; Becker, J. *J. Chem. Soc., Perkin Trans. 1* **1996**, 783.

- (11) SIR97: Altomare, A.; Burla, M. C.; Camalli, M.; Casciarano, G. L.; Giacovazzo, C.; Guagliardi, A.; Moliterni, A. G. G.; Polidori, G.; Spagna, R. *J. Appl. Crystallogr.* **1999**, *32*, 115.
 (12) *CrystalStructure 3.6.0: Crystal Structure Analysis Package*; Rigaku and Rigaku/MSC: 9009 New Trails Dr., The Woodlands TX 77381, 2000–2004.
 (13) Kobayashi, A.; Tanaka, H.; Kumasaki, M.; Torii, H.; Narymbetov, B.; Adachi, T. *J. Am. Chem. Soc.* **1999**, *121*, 10763.



^a Reagents and conditions: (i) 25 wt % tetramethylammonium hydroxide in methanol (4 equiv), dry THF, room temperature, 30 min, then $\text{NiCl}_2 \cdot 6\text{H}_2\text{O}$ (0.5 equiv), -78°C to room temperature, overnight. (ii) Electrochemical oxidation in MeCN solution containing $^t\text{Bu}_4\text{N}^+\text{PF}_6^-$ as a supporting electrolyte.

of $^t\text{Bu}_4\text{N}^+\text{PF}_6^-$ in dry acetonitrile under a constant current of $0.2 \mu\text{A}$. The comparatively air-stable plate-shaped dark brown crystals of **1** grew on the anode within 3–4 weeks.

Structural Characterization of $(^t\text{Bu}_4\text{N})[\text{Ni}(\text{dmstfdt})_2]$ (1**).** The molecular structure and packing diagram of **1** are shown in Figure 1. There are two crystallographically independent $[\text{Ni}(\text{dmstfdt})_2]^-$ anions (A and B) and two $^t\text{Bu}_4\text{N}^+$ cations in the unit cell (Figure 1a). Two S–Ni–S planes connected to the central nickel atom are slightly bent with respect to each other with small dihedral angles of 4.5° and 8.4° for A and B, respectively. In addition, the anions (A and B) have a slightly bent structure at the positions of selenium atoms of the STF part with dihedral angles of 6.4° and 4.5° for A and 3.4° and 9.7° for B. As shown in Figure 1b,c, the anions (A and B) are arranged alternately along the *a*-axis, and the molecular planes incline between the adjacent anions (A and B) with a dihedral angle of 42.6° to produce a weakly dimerized zigzag -ABA'B'- array. These arrays form an anion layer parallel to the *ac*-plane. These layers are separated by the bulky $^t\text{Bu}_4\text{N}^+$ cations. There are several intermolecular $\text{S} \cdots \text{S}(\text{Se})$ contacts between the anions of the neighboring zigzag arrays in addition to many contacts between the adjacent anions in the zigzag array, indicating a two-dimensional interaction in the anion layer (Figure 1c).

Electrical Resistivity of $(^t\text{Bu}_4\text{N})[\text{Ni}(\text{dmstfdt})_2]$ (1**).** The electrical resistivities of **1** were measured on the single crystals by a conventional four-probe method in the temperature range from 340 to 77 K as shown in Figure 2. The measurements were made along the two directions in the elongated thin plate of the crystal of **1**. The room-temperature conductivities (σ_{RT}) were ca. 0.2 S cm^{-1} along the long axis and $\approx 0.001 \text{ S cm}^{-1}$ perpendicular to the long axis in the elongated thin plate (Figure 2). Although the room-temperature resistivity is high, a weakly metallic behavior was observed above room temperature (inset of Figure 2). Below 280 K, the resistivity increased very slowly with a small estimated activation energy of 17 meV down to 147 K with decreasing temperature. Then, a sharp resistivity increase

showing the transition to an insulating state was observed at 147 K.

Considering the high room-temperature resistivity and the 1:1 stoichiometry of the complex, the metallic behavior was quite an unexpected result. We confirm that all crystals examined (four crystals) gave a similar behavior. Usually, the room-temperature conductivities (σ_{RT}) of metallic molecular conductors are larger than 10 S cm^{-1} , and those belonging to the intermediate group between metals and semiconductors have σ_{RT} of about 1 S cm^{-1} .^{14,15} The systems with σ_{RT} less than 0.1 S cm^{-1} are usually semiconducting (or insulating). Since the conductor with a small bandwidth (*w*) tends to be low-conducting ($\sigma = ne^2t/m^*$ and $m^* \propto w^{-1}$), the small σ_{RT} of **1** suggests its small bandwidth. On the other hand, it is well-known that the system with $w/U \approx 1$ exhibits intermediate behavior between those of conducting and nonconducting systems.¹⁶ Roughly speaking, the molecular conductor with a small bandwidth (e.g., $w < 0.2 \text{ eV}$) is usually nonmetallic. However, it might be possible that **1** shows the weakly metallic behavior even when the bandwidth is fairly small owing to the possible small *U* of the $[\text{Ni}(\text{dmstfdt})_2]^-$ anion.

Band Structure of $(^t\text{Bu}_4\text{N})[\text{Ni}(\text{dmstfdt})_2]$ (1**).** Since the weakly metallic behavior was observed around the room temperature, the band picture will be valid in the high-temperature region. The tight-binding band structure calculation of **1** was carried out from transfer integrals estimated on the basis of the simple extended Hückel approximation ($t = ES$, where *S* is the intermolecular overlap integral and $E \approx -10 \text{ eV}$) by use of Slater-type atomic orbitals.¹⁷ The $[\text{Ni}(\text{dmstfdt})_2]^-$ anions (A and B) have approximately a D_{2h} symmetry. The extended Hückel MO calculations suggested that the symmetries of the highest occupied molecular orbital (HOMO) and the lowest unoccupied molecular orbital (LUMO) were b_{1u} and b_{2g} , respectively, and the HOMO–LUMO energy gaps (ΔE_{HL}) to be 0.20 eV for anion A and 0.16 eV for anion B, which is consistent with the previously reported small ΔE_{HL} of $[\text{Ni}(\text{L})_2]$.² The band calculations were performed using these HOMOs, LUMOs, and ΔE_{HL} values. The magnitude of the largest transfer integrals (*t*) was less than $4 \times 10^{-2} \text{ eV}$ (Figure 3). Considering the metallic behavior around room temperature, the small intermolecular interactions are quite surprising and strongly suggest the exceptionally small effective *U* for the $[\text{Ni}(\text{dmstfdt})_2]^-$ anion. The band energy dispersion curves are shown in Figure 4a. There are eight energy branches. The upper three branches

- (14) Williams, J. M.; Ferraro, J. R.; Thorn, R. J.; Carlson, K. D.; Geiser, U.; Wang, H. H.; Kini, A. M.; Whangbo, M.-H. *Organic Superconductors (Including Fullerenes)*; Prentice Hall: New York, 1992.
- (15) Ishiguro, T.; Yamaji, K.; Saito, G. *Organic Superconductors*, 2nd ed.; Springer-Verlag: Berlin, 1998.
- (16) (a) Ouyang, J.; Dong, J.; Yakushi, K.; Takimiya, K.; Otsubo T. *J. Phys. Soc. Jpn.* **1999**, *68*, 3708. (b) Ouyang, J.; Yakushi, K.; Takimiya, K.; Otsubo T.; Tajima, H. *Solid State Commun.* **1999**, *110*, 63.
- (17) The extended Hückel molecular orbital calculations were performed by the use of Slater-type atomic orbitals. The valence shell ionization potential H_{ii} (eV) and the exponent ζ_i are -20.0 and 2.122 for Se 4s and -11.0 and 1.827 for Se 4p, -22.0 and 2.122 for S 3s and -10.5 and 1.827 for S 3p, -21.4 and 1.625 for C 2s and -11.4 and 1.625 for C 2p, -13.6 and 1.0 for H 1s, and -10.95 and 2.1 for Ni 4s and -3.74 and 2.1 for Ni 4p. The 3d orbital of Ni is represented by a linear combination of two Slater-type orbitals: H_{ii} , ζ_i , χ_{ii} , and χ_{ii} values are -10.58 , 5.75 , 0.5681 , 2.0 , and 0.6294 , respectively.

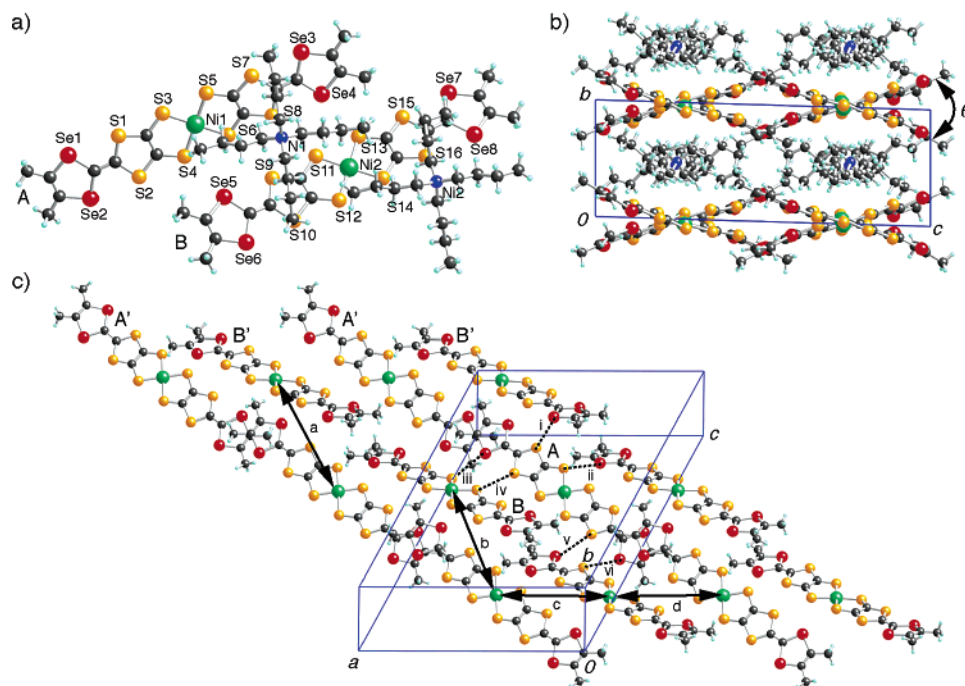


Figure 1. Crystal structure of $(\text{Bu}_4\text{N})[\text{Ni}(\text{dmstfdt})_2]$ (**1**) at room temperature. (a) Crystallographically independent molecules with labeling of the atoms. (b) Sandwiched structure of anion and cation layers. Two kinds of anions (A and B) form a zigzag -ABA'B'- array with dihedral angle (θ) of $42.6(1)^\circ$ between the adjacent anions (A and B) along the a -axis. (c) Anion layer in **1**. Intermolecular contacts (\AA): i, $\text{S7}\cdots\text{Se7}$, 3.723(6); ii, $\text{S5}\cdots\text{Se8}$, 3.795(5); iii, $\text{Se4}\cdots\text{S13}$, 3.638(6); iv, $\text{S8}\cdots\text{S11}$, 3.643(7); v, $\text{S2}\cdots\text{Se6}$, 3.693(6); and vi, $\text{Se2}\cdots\text{S10}$, 3.689(6). The Ni...Ni distances (\AA) are a, 14.436; b, 12.562; c, 9.747; and d, 9.813.

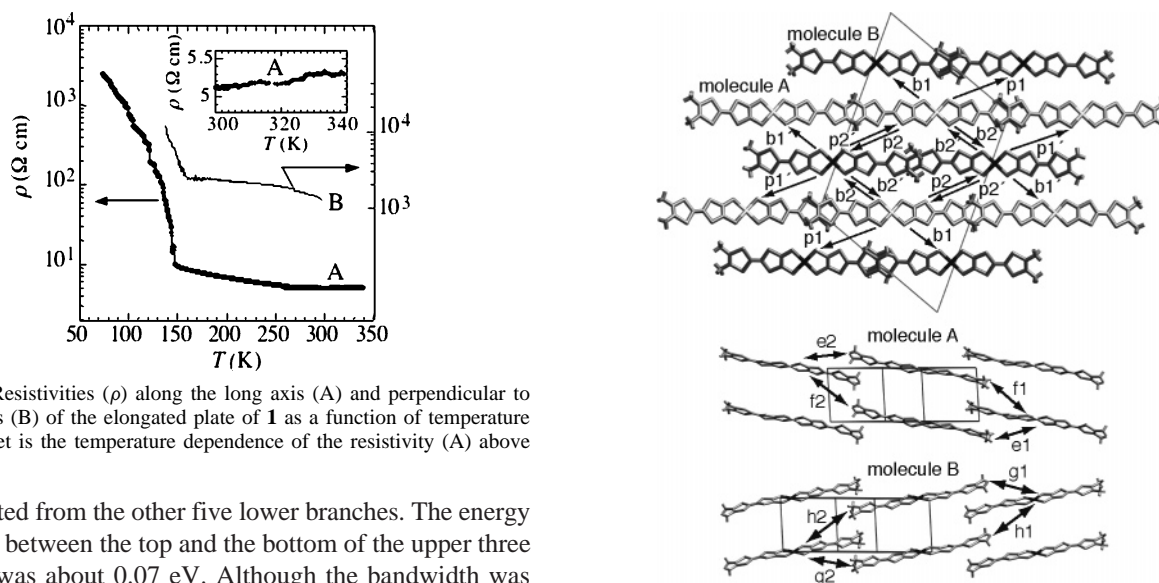


Figure 2. Resistivities (ρ) along the long axis (A) and perpendicular to the long axis (B) of the elongated plate of **1** as a function of temperature (T). The inset is the temperature dependence of the resistivity (A) above 300 K.

are separated from the other five lower branches. The energy difference between the top and the bottom of the upper three branches was about 0.07 eV. Although the bandwidth was very small, the band structure calculation based on the room-temperature crystal structure suggested the existence of electron and hole Fermi surfaces, which is consistent with the results of the resistivity measurements (Figure 4b).

Magnetic Properties of $(\text{Bu}_4\text{N})[\text{Ni}(\text{dmstfdt})_2]$ (1**).** Although the simple tight-binding band structure calculation gave results consistent with the weakly metallic behavior around room temperature, the 1:1 stoichiometry and small t suggested the possibility of the localization of conduction electrons due to the electron–electron correlation effect. Magnetic susceptibilities were measured on polycrystalline samples of the plate-like crystals using a SQUID magnetometer down to 2.0 K in the field of 10 kOe. The magnetic susceptibilities gradually increased from 340 K as the temperature decreased. A small anomaly was observed

Figure 3. Molecular arrangement and intermolecular overlap integrals of HOMOs and LUMOs. Overlap integrals ($\times 10^{-3}$) between molecule A and molecule B (HOMO \rightarrow HOMO, HOMO \rightarrow LUMO, LUMO \rightarrow HOMO, and LUMO \rightarrow LUMO) are b1 (−1.57, 2.42, 1.22, −1.61), b1' (−1.57, 1.22, 2.42, −1.61), b2 (−1.01, −1.32, −1.57, −1.84), b2' (−1.01, −1.57, −1.32, −1.84), p1 (1.04, −1.20, 1.21, −1.41), p1' (1.04, 1.21, −1.20, −1.41), p2 (3.07, 2.02, −1.36, −0.89), and p2' (3.07, −1.36, 2.02, −0.89). Overlap integrals ($\times 10^{-3}$) between same molecules (HOMO \rightleftharpoons HOMO, HOMO \rightleftharpoons LUMO, and LUMO \rightleftharpoons LUMO) are e1 (2.65, 3.20, 3.86), e2 (0.71, −0.29, 0.12), f1 (0.29, 0.32, 0.37), f2 (−0.026, 0.011, −0.005), g1 (2.06, −2.00, 1.94), g2 (0.73, 0.44, 0.27), h1 (0.28, −0.25, 0.23), and h2 (0.20, 0.12, 0.08). In these interactions (e1, ..., h2), HOMO \rightarrow LUMO and LUMO \rightarrow HOMO interactions are equal to each other.

around 150 K where the sharp transition to an insulator was observed (Figures 2 and 5a). Furthermore, another anomaly was observed around 20 K. The temperature dependence of the χT values is also given in Figure 5a. The magnitude of

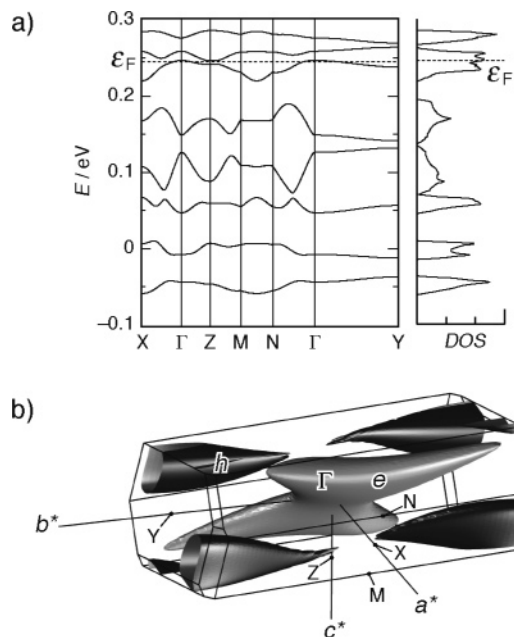


Figure 4. (a) Band dispersion and the density of state (DOS) for **1** calculated on the basis of the room-temperature crystal structure. (b) Calculated electron (*e*) and hole (*h*) Fermi surfaces.

the room-temperature paramagnetic susceptibility of $5.1 \times 10^{-4} \text{ emu mol}^{-1}$ is consistent with the paramagnetism due to the conduction electrons as expected from weakly metallic behavior around room temperature. But, the susceptibility behavior was far from that of Pauli paramagnetism. The χT values were almost linearly increased from 0.129 to 0.383 emu K mol^{-1} with decreasing temperature in the temperature range of 160–340 K. As mentioned before, $(^n\text{Bu}_4\text{N})[\text{Ni}(\text{dmstfdt})_2]$ (**1**) is a unique system with ambivalent character because it may be considered to be located near the boundary between the conductors and the insulators. The increase of χT suggests that the conduction electrons tend to be localized with lowering temperature at 160–280 K, where the resistivity increases gradually with decreasing temperature. The χT value was almost constant between 80 and 150 K. The constant χT value of $0.385 \text{ emu K mol}^{-1}$ corresponds to the theoretical value $[= N_{\text{Ag}} g^2 \mu_{\text{B}}^2 S(S+1)]$ calculated for the $S = 1/2$ localized spin with the g -value of 2.027 given by ESR measurements. The magnetic susceptibilities between 80 and 150 K were well-fitted by the Curie–Weiss law: $\chi = C/(T - \theta)$ giving $C = 0.383 \text{ emu K mol}^{-1}$ and $\theta = -4 \text{ K}$. Thus, it may be said that **1** undergoes a transition to an insulating state as a result of localization of the conduction electrons. $(^n\text{Bu}_4\text{N})[\text{Ni}(\text{dmstfdt})_2]$ (**1**) is a novel molecular conductor that shows the characteristic susceptibility changes suggesting the gradual electron localization from the high-temperature weakly metallic state to the low-temperature localized spin state. In spite of the possible small effective U , the electron correlation will be very important in this system because of small t values obtained by the extended Hückel calculations (Figure 3).

The field dependence of magnetization of a polycrystalline sample was measured at 2.0 K. The magnetization shows a prominent hysteresis between $\pm 7.5 \text{ kOe}$ with a coercive field of 1.3 kOe; at higher fields, it is reversible and linear up to the maximum of $\pm 50 \text{ kOe}$ (Figure 5b). This behavior is

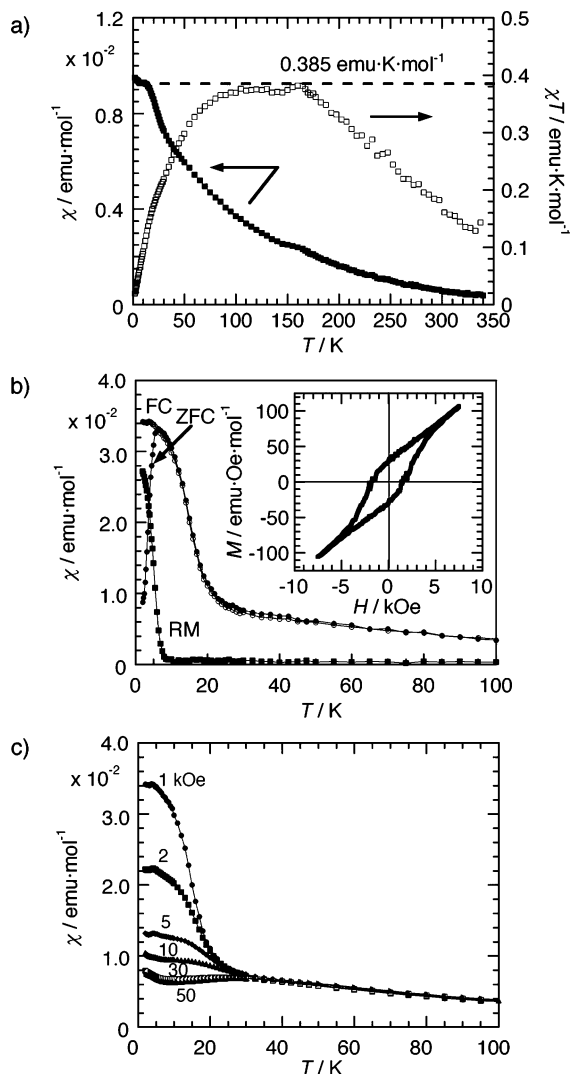


Figure 5. (a) Temperature (T) dependence of magnetic susceptibility (χ) of the polycrystalline sample of **1** under the magnetic field of $H = 10 \text{ kOe}$. The χT vs. T plot is also depicted in Figure 5a. The dotted line ($0.385 \text{ emu K mol}^{-1}$) is the theoretical χT value estimated for a paramagnet with $S = 1/2$ and $g = 2.027$. (b) The zero-field-cooled (ZFC) and field-cooled (FC) susceptibilities and remnant magnetization (RM) as a function of temperature (T) in a field of 1 kOe for the polycrystalline sample of **1**. The inset shows the field (H) dependence of the magnetization (M) at 2.0 K. (c) Temperature (T) dependence of the FC susceptibilities (χ) of **1** under various magnetic fields.

typical of a weak ferromagnet, where the remnant magnetization is related to the canted moment and gives an estimated canting angle of less than 1° . The zero-field-cooled (ZFC), field-cooled (FC), and remnant magnetizations of the polycrystalline sample in a field of $H = 1 \text{ kOe}$ indicate an unusual blocking of the moments only below 7 K, which is well below the Néel temperature of 20 K. Figure 5c shows the temperature dependence of the FC susceptibilities under various magnetic fields; it is found to be very dependent on the applied field as expected for a canted antiferromagnet.

Crystal Structure of $(^n\text{Bu}_4\text{N})[\text{Ni}(\text{dmstfdt})_2]$ (**1**) at 90 K.

To investigate the origin of the semiconductor-to-insulator transition, the crystal structure analyses of **1** were performed at three different temperatures: 280, 200, and 90 K. The presence of the structural phase transition of **1** was confirmed between 90 and 200 K, where the change of the space group from $P\bar{1}$ at high temperature to $P2_1/a$ at low temperature,

and the increase of the lattice constant b from 8.661(3) to 17.167(8) Å took place.¹⁸ Two [Ni(dmstfdt)₂][−] anions (here, we label them C and D to prevent confusion with the earlier description) and two ⁿBu₄N⁺ cations are crystallographically independent at 90 K. The [Ni(dmstfdt)₂][−] anions (C and D) have a slightly nonplanar molecular structure similar to those at room temperature, but the planarity of anion C is relatively high as compared with those of the other anions (A, B, and D). Although the [Ni(dmstfdt)₂][−] anions form the zigzag one-dimensional array along the a -axis in the same way as the situation at room temperature, each zigzag array is constructed with the same kind of the crystallographically independent anion (C or D) unlike the -ABA'B'- arrangement at room temperature. The dihedral angles between neighboring anions in the zigzag arrangement are 44.4(5)° for the anion C array and 55.5(5)° for the anion D array, respectively. A band dispersion and Fermi surface were also calculated on the basis of the crystal structure at 90 K.¹⁸ The HOMO–LUMO energy gap of the planar anion C (0.401 eV) is larger than that of anion D (0.125 eV). The band derived from the LUMO of anion C isolates above the Fermi level, resulting in the vanishing of the Fermi surface at 90 K, which is consistent with the insulating state of complex **1**.

As mentioned before, (ⁿBu₄N)[Ni(dmstfdt)₂] (**1**) exhibits weak ferromagnetism at low temperature. It is well-known that the Dzyaloshinsky–Moriya (DM) interaction¹⁹ causes the weak ferromagnetism, when the inversion center is absent

between the spin sites of the two sublattices of the AF state. In the case of **1**, this condition is satisfied if one associates the C and D arrays to the two sublattices where the two independent anions are not related by an inversion.

Conclusion

(ⁿBu₄N)[Ni(dmstfdt)₂] (**1**) is a unique ambivalent molecular system exhibiting weakly metallic behavior above room temperature despite the 1:1 stoichiometry and weak ferromagnetism of localized spins at low temperature. The small calculated intermolecular transfer integrals and weakly metallic behavior suggest that the effective on-site Coulombic repulsion is very small, which will be due to the delocalization of π -frontier electrons over the left and right extended–TTF ligands. The temperature dependence of the susceptibility is also very unique, which indicated the gradual increase of the localized magnetic moments associated with the slow increase of the resistivity with lowering the temperature in the range of 160–280 K. Below the insulating transition temperature ($T < 150$ K), the electrons are localized one per [Ni(dmstfdt)₂] molecule resulting in $S = 1/2$. The compound further exhibits long-range magnetic ordering with a Néel ground state below 20 K and a small canting possibly due to Dzyaloshinsky–Moriya (DM) interactions. It also displays an unusual magnetic hardness only below 7 K reaching 1.3 kOe at 2.0 K.

Acknowledgment. This work was financially supported by a Grant-in-Aid for Scientific Research (S) (14103005), Priority Areas of Molecular Conductors (15073209), and 21st Century COE Program for Frontiers in Fundamental Chemistry from the Ministry of Education, Culture, Sports, Science and Technology. This work was also supported by CREST (Core Research for Evolutional Science and Technology) of JST (Japan Science and Technology Agency). The authors are grateful to Prof. H. Fukuyama of Tokyo University of Science, Prof. C. Terakura of Hokkaido University, and Prof. M. Kurmoo of Université Louis Pasteur, Institut Le Bel for their encouragement and discussions and also thank Prof. Y. Nakazawa of Osaka University for useful discussions about weak ferromagnetism.

Supporting Information Available: X-ray crystallographic files in CIF format. This material is available free of charge via the Internet at <http://pubs.acs.org>.

CM062131Q

(18) Crystal data at 90 K: C₃₂H₄₈NNiS₈Se₄; $M = 1077.76$; monoclinic; space group $P2_1/a$ (No. 14); $a = 19.879(11)$, $b = 17.167(8)$, and $c = 25.55(1)$ Å; $\beta = 112.315(3)^\circ$; $V = 8065.5(74)$ Å³; $Z = 8$; $d_{\text{calcd}} = 1.775$ g cm^{−3}; $\mu = 45.32$ cm^{−1}; and $F_{000} = 4312.00$. The number of collected reflections was 55786. The structure was solved by direct methods (SIR97). The atomic scattering factors were taken from the International Tables for X-ray Crystallography. The non-hydrogen atoms were anisotropically refined by a full-matrix least-squares method based on 7226 observed reflections [$I > 4.0\sigma(I)$] and 765 variable parameters. The final R and GOF values are $R = 0.100$, $R_w = 0.131$, and GOF = 1.344. All calculations were performed using the CrystalStructure crystallographic software package. The low-temperature crystal structure analysis revealed a structural phase transition around 150 K. But, similar to the room-temperature structure, there are two crystallographically independent molecules in the low-temperature structure, which is consistent with the possibility of spin canting. However, probably due to the large structure change, the crystal quality was heavily deteriorated, which prevented us from obtaining sufficiently accurate structure data.

(19) (a) Dzyaloshinsky, I. *J. Phys. Chem. Solids* **1958**, *4*, 241. (b) Moriya, T. *Phys. Rev.* **1960**, *120*, 91.